Kranias, E. G. (1985a) *J. Biol. Chem. 260*, 11006–11010.
Kranias, E. G. (1985b) *Biochim. Biophys. Acta 844*, 193–199.
Laemmli, U. K. (1970) *Nature (London) 227*, 680–685.
Lamers, J. M. H., & Stinis, H. T. (1980) *Biochim. Biophys. Acta 624*, 443–459.
Lau, Y. H., Caswell, A. H., Garcia, M., & Letellier, L. (1979) *J. Gen. Physiol. 74*, 335–349.
Le Peuch, C. J., Haiech, J., & Demaille, J. G. (1979) *Biochemistry 18*, 5150–5157.
Le Peuch, C. J., Le Peuch, D. A. M., & Demaille, J. G. (1980) *Biochemistry 19*, 3368–3373.
Louis, C. F., Maffitt, M., & Jarvis, B. (1982) *J. Biol. Chem. 257*, 15182–15186.
Lowry, O. H., Rosebrough, N. J., Farr, A. L., & Randall, R. J. (1951) *J. Biol. Chem. 193*, 265–275.
Movesian, M. A., Nishikawa, M., & Adelstein, R. S. (1984) *J. Biol. Chem. 259*, 8029–8032.
Niggli, V., Penniston, J. T., & Carafoli, E. (1979) *J. Biol. Chem. 254*, 9955–9958.
Pharmacia Fine Chemicals (1982) *Isoelectric Focusing, Principles & Methods*, Ljunforetagen AB, Uppsala, Sweden.
Schwartz, A., Entman, M. L., Kaniike, K., Lane, L. K., Winckle, W. B. V., & Bornet, E. P. (1976) *Biochim. Biophys. Acta 426*, 57–72.
Stadle, J. M., Nambi, P., Shorr, R. G. L., Sawyer, D. F., Caron, M., & Lefkowitz, R. J. (1983) *Proc. Natl. Acad. Sci. U.S.A. 80*, 3173–3177.
Tada, M., Kirchberger, M. A., & Katz, A. M. (1975) *J. Biol. Chem. 250*, 2640–2647.
Tada, M., Ohmori, F., Yamada, M., & Abe, H. (1979) *J. Biol. Chem. 254*, 319–326.
Tada, M., Inui, M. Yamada, M., Kadoma, M., Kuzuya, T., Abe, H. & Kakiuchi, S. (1983) *J. Mol. Cell. Cardiol. 15*, 335–346.
Wegener, H. L., & Jones, L. R. (1984) *J. Biol. Chem. 259*, 1834–1841.
Will, H., Levchenko, T. S., Levitsky, D. O., Smirnov, V. N., & Wollenberger, A. (1978) *Biochim. Biophys. Acta 543*, 175–193.
Wharton, D. C., & Griffiths, D. E. (1962) *Arch. Biochem. Biophys. 96*, 103.
Wray, H. L., Gray, R. R., & Olsson, R. A. (1973) *J. Biol. Chem. 248*, 1496–1498.

Rapid Filtration Study of the Phosphorylation-Dependent Dissociation of Calcium from Transport Sites of Purified Sarcoplasmic Reticulum ATPase and ATP Modulation of the Catalytic Cycle†

Philippe Champeil* and Florent Guillain
Service de Biophysique, Département de Biologie, CEN Saclay, 91191 Gif-sur-Yvette Cedex, France
Received May 12, 1986; Revised Manuscript Received August 20, 1986

ABSTRACT: Time-resolved filtration measurements using radioactive calcium were conducted to investigate with leaky preparations the kinetic features of the dissociation of transported calcium to the luminal side of the sarcoplasmic reticulum calcium pump, which occurs concomitantly with isomerization of the phosphorylated ATPase. At pH 6 and 20 °C, Ca^{2+} dissociation was moderately fast in the absence of potassium (3–5 s^{-1} at 0.05 mM ATP), implying that the dephosphorylation step (about 1.5 s^{-1}) was the main contributor to rate limitation under these conditions. Potassium slowed down Ca^{2+} release but stimulated dephosphorylation, so that in its presence Ca^{2+}-releasing isomerization did contribute to rate limitation, especially at neutral pH. At pH 6 in the absence of potassium and in the presence of magnesium, millimolar concentrations of ATP doubled the rate of Ca^{2+} dissociation, as also shown by dual-wavelength detection of fast changes in the absorbance of the Ca^{2+}-sensitive dye Antipyrylazo III. Under the same conditions, low-affinity binding of ATP to phosphoenzyme was demonstrated. It is suggested that this low-affinity acceleration by ATP of the crucial step leading to dissociation of transported Ca^{2+} is the specific interaction responsible for the low-affinity acceleration of overall ATPase activity generally observed in the presence of potassium at neutral pH. Hydrolysis of the Ca^{2+}-deprived phosphoenzyme was accelerated by ATP in the absence but not in the presence of Mg^{2+} in the dephosphorylation medium. We suggest that metal-free ATP is a more potent activator than Mg·ATP for transitions involving phosphoenzyme.

The membranous sarcoplasmic reticulum ATPase[1] catalyzes ATP-dependent active transport of calcium from the cytoplasm to the reticular lumen. When the catalytic cycle is initiated by adding Mg·ATP to Ca^{2+}-saturated ATPase, phosphoenzyme is formed at a fast rate; thereafter, a conformational transition of the phosphorylated ATPase occurs together with diminution of the affinity for calcium of the transport sites, and the bound calcium ions dissociate to the lumen of the SR vesicles. Later, the covalent acyl–phosphate bond in the phosphoenzyme is hydrolyzed, and the ATPase conformation reverts to the initial one to which cytoplasmic calcium may

† A preliminary communication has been presented at the 30th Biophysical Society Meeting in San Francisco (Champeil & Guillain, 1986).

[1] Abbreviations: ATPase, adenosinetriphosphatase; SR, sarcoplasmic reticulum; Mops, 4-morpholinepropanesulfonic acid; Mes, 2-(*N*-morpholino)ethanesulfonic acid; Tes, 2-[[tris(hydroxymethyl)methyl]-amino]ethanesulfonic acid; EGTA, ethylene glycol bis(β-aminoethyl ether)-*N*,*N*,*N*′,*N*′-tetraacetic acid; Tris, tris(hydroxymethyl)aminomethane; ATP, adenosine triphosphate; PCA, perchloric acid; k_{obsd}, observed rate constant; A_{23187}, calcimycin; P_i, inorganic phosphate; Me_2SO, dimethyl sulfoxide.

0006-2960/86/0425-7623$01.50/0

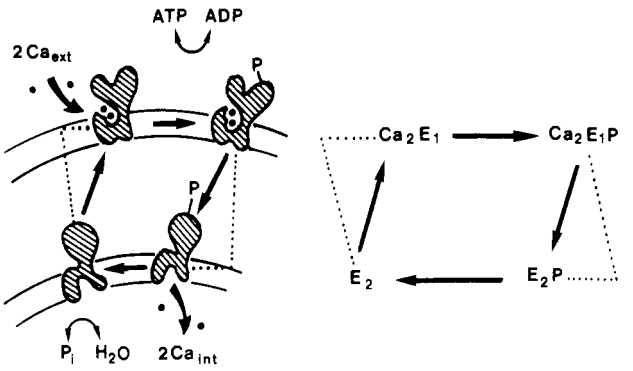

FIGURE 1: Simplified description of the four-intermediates reaction scheme considered here. Dotted lines were superimposed to indicate that both the calcium-releasing phosphoenzyme isomerization and the Ca^{2+} binding induced transition comprise several substeps. However, we make no assumption here about the relative rates of the conformational changes vs. the rates of release or binding.

bind again. Figure 1 depicts a simplified reaction scheme for the ATPase cycle, which is basically the one put forward by Makinose (1973) and includes two major conformations whose interconversion is the essence of the transport mechanism (de Meis & Vianna, 1979). In the first (E_1) conformation, the ATPase Ca^{2+} sites face the cytoplasm, and the ATPase can be phosphorylated by ATP, resulting in the formation of an ADP-sensitive phosphoenzyme (Ca_2E_1P); in the second (E_2) conformation, the Ca^{2+} sites face the lumen, and the ATPase can be phosphorylated by P_i, resulting in a water-sensitive but ADP-insensitive phosphoenzyme (E_2P).

Diminution of the affinity for calcium induced by phosphorylation of the ATPase combined with the topological reorientation of the transport sites is a necessary and key step in any active transport mechanism. However, in spite of an early demonstration with leaky ATPase of Ca^{2+} dissociation resulting from this diminution of affinity (Ikemoto, 1975), it was only recognized in 1981 that in order to make the dissociation observable, the late steps in the cycle (dephosphorylation from E_2P to E_2 and conversion from E_2 to Ca_2E_1) had to be rendered the slowest ones in the cycle, for instance, by including Me_2SO in the medium, thus allowing Ca^{2+}-free species to accumulate at steady state (Watanabe et al., 1981). Meanwhile, the transition from ADP-sensitive to ADP-insensitive phosphoenzyme had been documented in studies performed at low temperatures (Shigekawa & Dougherty, 1978; Shigekawa & Akowitz, 1979). These studies were extended (Takisawa & Tonomura, 1979; Yamada & Ikemoto, 1980; Nakamura & Tonomura, 1982; Inesi et al., 1982; Nakamura, 1983; Dean & Gray, 1983; Takisawa & Makinose, 1983; Shigekawa et al., 1983; Andersen et al., 1985b; Froehlich & Heller, 1985), and the transition also proved detectable by measuring changes in H^+ binding (Yamaguchi & Kanazawa, 1984, 1985), in the tryptic cleavage pattern (Andersen et al., 1985a) and in intrinsic fluorescence (Fernandez-Belda et al., 1984; Andersen et al., 1985b).

Despite the large body of data that has accumulated, there is still much to learn about this crucial isomerization resulting in calcium dissociation, especially about its kinetic features at room temperature. The initial purpose of the present investigation was to document this issue, using leaky ATPase preparations and either radioactive calcium together with a newly designed Biologic rapid filtration system or optical detection of the Ca^{2+} release. Our results, mostly obtained at 20 °C, were in general agreement with what could be inferred from previous investigations, most of them performed at low temperature. In addition, we demonstrated low-affinity acceleration by ATP of Ca^{2+} dissociation. We then enlarged the scope of this investigation to further document the modulatory effect of ATP on the other steps in the ATPase reaction cycle and to sort out which step contributed to rate limitation under a given experimental condition. We concluded that the low-affinity interaction of ATP with the calcium-containing phosphoenzyme (Ca_2E_1P in our simplified scheme) was the critical event responsible for the overall ATP hydrolysis activation generally observed at millimolar ATP concentrations in standard mediums (e.g., potassium-containing mediums buffered near neutrality). The calcium-deprived phosphoenzyme (E_2P) also interacted with nucleotides; metal-free ATP was, however, a better activator than Mg·ATP to promote dephosphorylation.

Experimental Procedures

Sarcoplasmic reticulum vesicles (SR) were prepared from rabbit skeletal muscle as previously descrived (Champeil et al., 1985), and purified Ca^{2+}-ATPase membranes were prepared from SR by treatment with a low concentration of deoxycholate according to Meissner et al. 1973). This treatment resulted in satisfactory purification of the ATPase and in a correspondingly high concentration of active sites (see Figure 8 below), but calcium ions did not leak freely out of this "purified ATPase" preparation. The residual impermeability was more apparent at acidic pH; at pH 6, total abolition of residual uptake and therefore full expression of steady-state phosphorylation-dependent calcium dissociation required the addition of a relatively large amount of the Ca^{2+} ionophore A_{23187}, typically, 4 g of ionophore/100 g of protein (data not shown). Note that, when the ionophore was used at such high concentrations, it probably behaved to some extent like a nonsolubilizing but perturbing detergent (McIntosh & Davidson, 1984; Champeil et al., 1986); this was reflected in some slowing down of the ATP hydrolysis rate, which in turn resulted from the slowing down of the dephosphorylation rate (see legend to Figure 9). We do not know why our ATPase preparation was not completely leaky; it might be connected with less efficient delipidation than previously reported. The implications of the purified ATPase's residual impermeability for the study of Ca^{2+} release will be discussed later.

Note that once the ionophore was added either to the purified ATPase or to SR vesicles, it could not be removed from the membrane by simply rinsing with ionophore-free medium for several seconds (data not shown). This slow "OFF rate" for the incorporated ionophore has practical implications, as shown below.

^{45}Ca, [^{32}P]P_i, or [^{32}P]ATP binding to the ATPase was measured with Millipore cellulose ester filters (HA 0.45 μm) on which the ATPase was adsorbed (Dupont, 1980). Such measurements require estimation of the amount of substrate that is trapped in the filter with water but not bound to the ATPase. Generally, this amount is determined by pouring the radioactive solution through the filter in the absence of membranes. Here, however, in order to determine the volume of the solution trapped, we preferred to include [^{3}H]sucrose in the substrate-containing solution. In the absence of membranes, we found no evidence of any nonspecific binding of $^{45}Ca^{2+}$, [^{32}P]P_i, or [^{32}P]ATP to the filter in excess of the trapped volume, and the double-labeling procedure made the measurement of protein-bound substrate more precise.

Time-resolved measurements of dissociation or binding were performed with the Biologic rapid filtration system (Dupont, 1984). A Millipore HA filter was first loaded with 0.3 mg of protein to which 4% w/w A_{23187} had already been added. Note that in the absence of membrane free ionophore binds

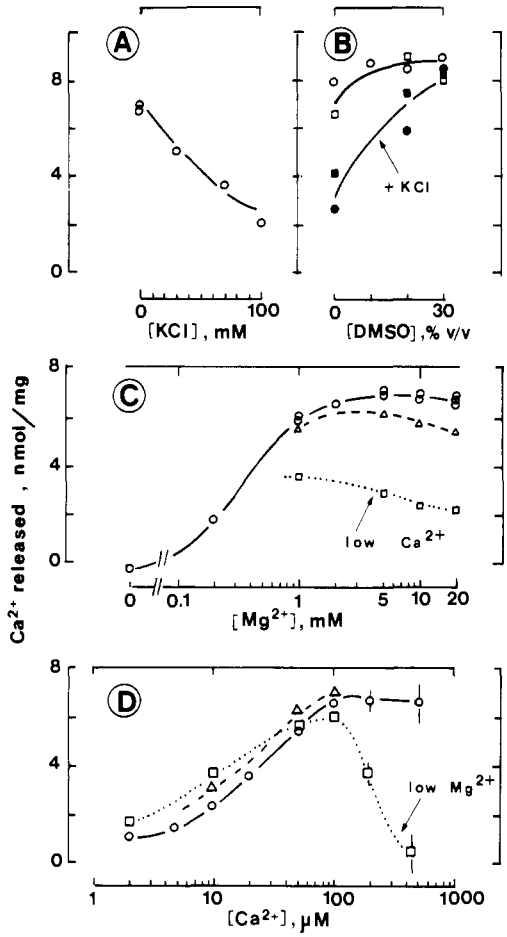

FIGURE 2: Steady-state phosphorylation-induced Ca^{2+} dissociation at pH 6 under various conditions, as deduced from ^{45}Ca filtration experiments. A total of 1 mL of a solution containing 150 mM Mes–Tris, 20 mM Mg^{2+}, 0.1 mM $^{45}Ca^{2+}$, 1 mM [^{3}H]sucrose, 0.3 mg/mL ATPase, and 0.012 mg/mL A_{23187} (4% w/w) was first filtered through a Millipore HA filter. (A and B) The filter was then rinsed with 1 mL of a similar solution without ionophore but containing various proportions of KCl and of Mes–Tris ranging from no KCl and 150 mM Mes–Tris to 100 mM KCl and 30 mM Mes–Tris (panel A) or containing various percentages (v/v) of Me_2SO (panel B) in the absence (open symbols)or presence (closed symbols) of potassium. This filter was counted. After similar treatment, an identical filter was submitted to an additional perfusion with a medium containing ATP at a concentration of 0.05 (circles in panel A), 0.1 (circles in panel B), or 1 mM (squares in panel B); the filter was counted. Subtraction yielded the drop in the amount of bound calcium, which was plotted here as calcium released. (C) The ATPase adsorbed on the filter was perfused with a potassium-free medium in the presence of various concentrations of Mg^{2+} and otherwise processed as in panel A. The perfusion medium contained a calcium concentration of 0.1 (circles), 0.05 (triangles), or 0.01 mM (squares). (D) The ATPase adsorbed on the filter was perfused with a potassium-free medium in the presence of various concentrations of Ca^{2+} and otherwise processed as in panel A. The perfusion medium contained a magnesium concentration of 20 (circles), 5 (triangles), or 1 mM (squares).

efficiently to the cellulose ester filters (this can be deduced from the absence of ionophore fluorescence in the filtrate); however, due to the slow OFF rate for membrane-incorporated ionophore, previously treated ATPase membranes layered on the filter remained leaky during the time required for the filtration experiment. After being loaded, the filter was perfused with a substrate-containing but ionophore-free medium during a preset period ranging from 25 ms to 10 s. The filter was then counted in a scintillation mixture.

Steady-state covalent ^{32}P-labeled phosphoenzyme formation was measured by filtration on a glass fiber filter after acid quenching (Champeil et al., 1985).

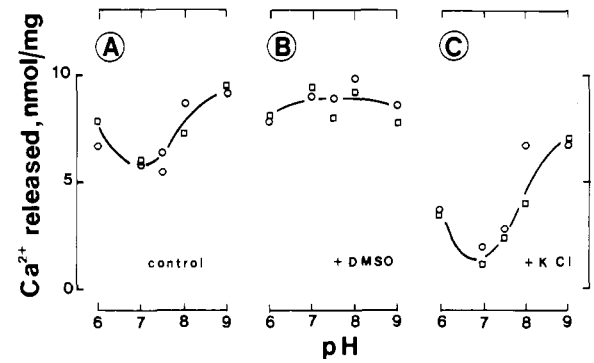

FIGURE 3: pH dependence of the amount of phosphorylation-dependent Ca^{2+} dissociation at steady state in the presence of 10 mM Mg^{2+}, 0.05 mM $^{45}Ca^{2+}$, 0.5 mM [^{3}H]sucrose, and either 165 mM buffer and no KCl or Me_2SO (panel A), 130 mM buffer and 20% Me_2SO (panel B), or 30 mM buffer and 100 mM KCl (panel C). The ATP concentration was 0.05 (circles) or 5 mM (squares). The buffers used were Mes (pH 6), Mops (pH 7), Tes (pH 7.5), Tricine (pH 8)—all of them adjusted with Tris—or Tris (pH 9)—which was adjusted with HCl. Experimental procedure was as for Figure 2.

The Ca^{2+} dye Antipyrylazo III (Fluka) was also used to detect ATP-induced Ca^{2+} release, since it produced larger changes in optical density than murexide and since in our hands the use of Arsenazo III led to phosphorylation-related artifacts (Riollet and Champeil, submitted for publication). In kinetic measurements, the Dionex stopped-flow system was used together with its dual-detector D-137 attachment, in order to resolve the rate of Ca^{2+} dissociation. Several traces were accumulated and averaged to improve the signal to noise ratio.

All experiments except those depicted in Figure 6A were performed at 20 °C. The reaction medium investigated in the greatest detail contained 150 mM Mes buffer, titrated to pH 6.0 with Tris, and no monovalent cations. To this medium were added Ca^{2+}, Mg^{2+}, EGTA, KCl, Me_2SO, and ATP as indicated in the figure legends.

RESULTS

Steady-State Calcium Dissociation. Phosphorylation-dependent dissociation of calcium from the ATPase transport sites was estimated as follows: leaky ATPase membranes were adsorbed on a Millipore filter and perfused for 5–10 s with a calcium-containing medium, and the amount of passively bound calcium was measured. A total of 11–15 nmol of Ca^{2+} binding sites/mg of protein was titrated. Another filter on which the same amount of ATPase had been adsorbed was then perfused with the same calcium-containing solution to which substrate had been added, and the calcium bound to the ATPase under these steady-state conditions was again measured; under these conditions, less calcium was bound to the ATPase, due to accumulation of Ca^{2+}-free ATPase intermediates during ATP hydrolysis; the substrate-dependent drop in bound calcium, obtained by subtraction, was plotted in Figures 2 and 3 as "calcium released".

Figure 2A shows that at pH 6 and 20 °C the amount of calcium released was reduced by potassium; it was enhanced by Me_2SO, both in the absence (open symbols) and in the presence (closed symbols) of potassium (Figure 2B). Figure 2C shows that Mg^{2+} was necessary to make this Ca^{2+} release observable. The smaller Ca^{2+} release observed at high Mg^{2+} but low Ca^{2+} concentrations (squares) reflected the lower ATPase affinity for Ca^{2+} in the presence of magnesium (Guillain et al., 1982). Figure 2D shows that at low magnesium concentrations (squares) an unduly high Ca^{2+} concentration was inhibitory, probably due to competition between Ca·ATP and Mg·ATP for the phosphorylation site (see Figure

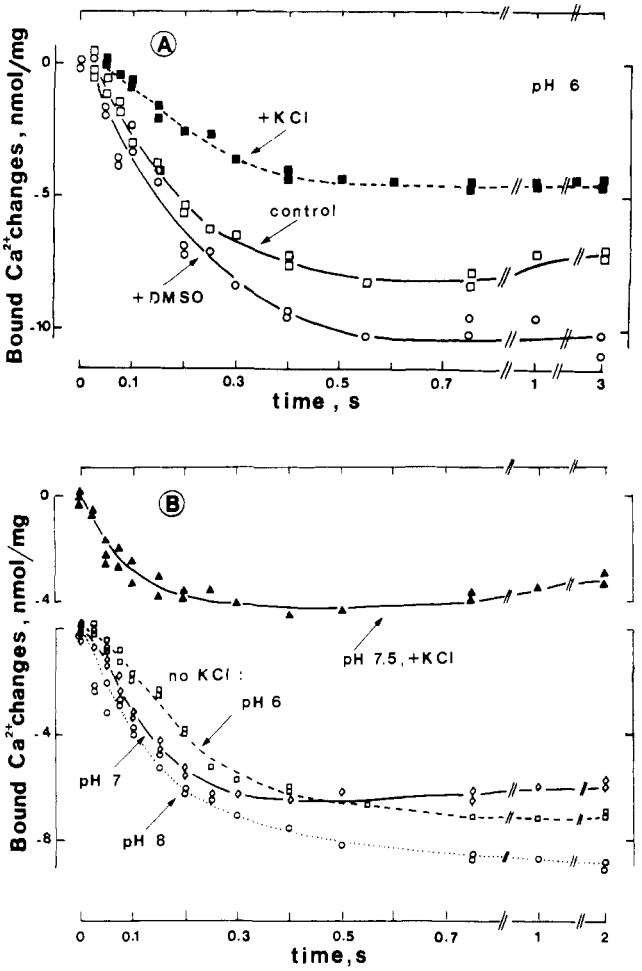

FIGURE 4: Rate of phosphorylation-dependent Ca^{2+} dissociation, measured in various mediums by rapid filtration. Purified ATPase was preincubated with 4% w/w ionophore, layered on a filter, and perfused with the appropriate solution in the absence of ATP in order to measure the amount of Ca^{2+} passively bound, i.e., bound at time zero. An additional perfusion in the presence of ATP for predetermined periods was performed with the Biologic rapid filtration system. In panel A, as in Figure 2A,B, the perfusion medium contained 20 mM Mg^{2+}, 0.1 mM Ca^{2+}, 0.05 mM ATP (pH was adjusted to 6.0), and 150 mM Mes–Tris (open squares), 100 mM KCl and 45 mM Mes–Tris (closed squares), or 130 mM Mes–Tris and 20% v/v Me_2SO (open circles). In panel B, as in Figure 3, the perfusion medium contained 10 mM Mg^{2+}, 0.05 mM Ca^{2+}, 0.05 mM ATP, and 165 mM Mes–Tris (pH 6, open squares), 165 mM Mops–Tris (pH 7, open diamonds), 165 mM Tricine–Tris (pH 8, open circles), or 100 mM KCl and 30 mM Tes–Tris (pH 7.5, closed triangles).

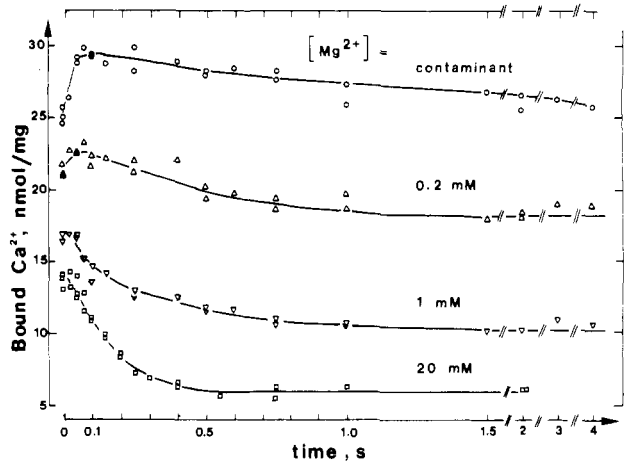

FIGURE 5: Magnesium dependence of the rate and extent of Ca^{2+} dissociation at pH 6, in the absence of potassium. This experiment was similar to the one in Figure 4, but the amount of Ca^{2+} bound was plotted instead of the changes in Ca^{2+} binding, thus showing the initial nonspecific Ca^{2+} binding in the absence of magnesium. In addition to 180 mM Mes–Tris (pH 6), 1 mM [^{3}H]sucrose, 0.1 mM $^{45}Ca^{2+}$, and 0.05 mM ATP, the perfusion medium contained various amounts of magnesium: 20 (squares), 1 (upside-down triangles), 0.2 (ordinary triangles), or 0 mM (circles).

5). Large amounts of Ca^{2+} were also released when the catalytic cycle was initiated by adding 1 mM acetyl phosphate (not shown). The results in Figure 2 was consistent with what has been previously deduced by other groups from ADP-sensitivity experiments at low temperature or direct calcium binding measurements [see, for instance, Shigekawa and Akowitz (1979), Takisawa and Tonomura (1979), Watanabe et al. (1981), Nakamura and Tonomura (1982), Shigekawa et al. (1983), and Andersen et al. (1985b)].

The pH dependence of calcium dissociation was also tested under different conditions, in the absence of both potassium and Me_2SO (Figure 3A), in the absence of potassium but in the presence of Me_2SO (Figure 3B), or in the absence of Me_2SO but in the presence of potassium (Figure 3C). We confirmed the trend toward a large Ca^{2+} release previously observed at alkaline pH (Takisawa & Tonamura, 1983; Nakamura & Tonomura, 1982; Andersen et al., 1985b). However, the minimal Ca^{2+} release observed at neutral pH (Figure 3A,C) is a novel feature of this investigation, which we believe highly significant and completely consistent with accumulated knowledge about the various steps in the cycle (see below and Discussion).

Kinetics of Phosphorylation-Dependent Ca^{2+} Dissociation: Rapid Filtration Experiments. Figures 4 and 5 show that the use of the Biologic rapid filtration system allowed resolution of ATP-induced Ca^{2+} dissociation under various conditions. At pH 6, the presence of Me_2SO (circles in Figure 4A) did not greatly affect the initial rate of Ca^{2+} release; in contrast, the presence of KCl (closed squares in Figure 4A) significantly reduced this rate, thus contributing to the KCl-induced shift toward Ca_2E_1P previously observed in the steady state. In Figure 4B, it is shown that the rate of Ca^{2+} dissociation was only moderately faster at pH 7 and 8 than at pH 6 (compare diamonds and circles to squares). The final levels observed in these kinetic experiments (Figure 4) were consistent with the steady-state data in the previous section (Figures 2 and 3).

Figure 5 depicts an experiment performed at pH 6 in the presence of magnesium (circles). Passive binding at time zero, before addition of ATP, rose to high values in the absence of magnesium, evidently due to calcium binding to nonspecific anionic sites on the ATPase (and perhaps also to the ionophore trapped in the filter). In this case, after ATP perfusion was initiated, rapid filtration measurements clearly revealed both the occurrence of Ca·ATP binding suspected by Dupont (1980) and the slowing down of the transition to a Ca^{2+}-depleted phosphoenzyme (circles in Figure 5).

ATP Modulation of the Rate of Ca^{2+} Dissociation. The most significant outcome of the present series of experiments was the fact that high concentrations of ATP moderately but definitely accelerated the rate of calcium dissociation. This was observed at pH 6 under various conditions, two of which are shown in Figure 6, at 5 °C in the absence of potassium and Me_2SO (panel A) and at 20 °C in the presence of potassium and Me_2SO (panel B). In both cases, 5 mM ATP (squares) induced much faster Ca^{2+} release than 0.05 mM ATP (circles). At the latter concentration, enzyme phosphorylation from ATP, which precedes the Ca^{2+}-releasing step, is already fast enough to prevent unduly slow phosphorylation

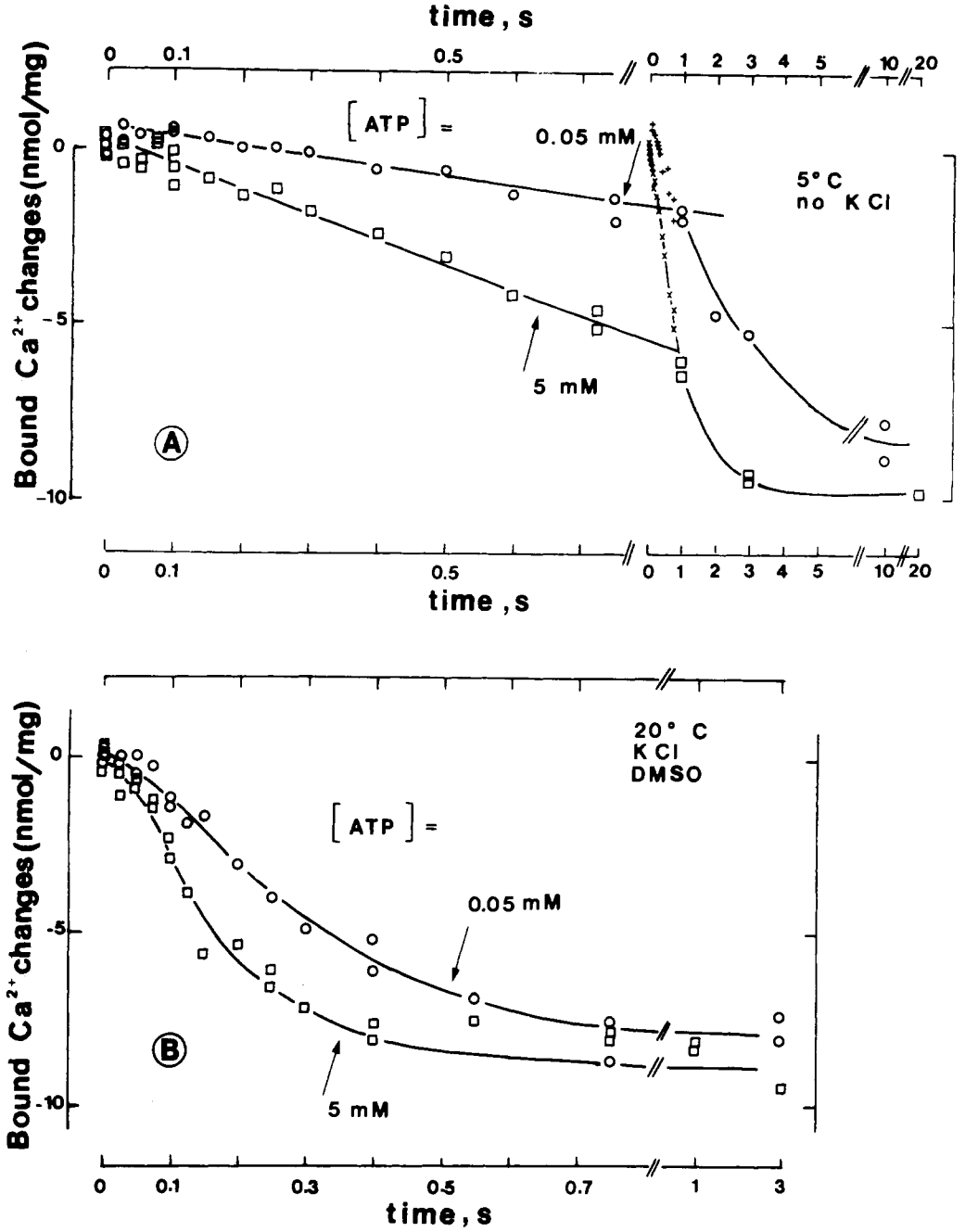

FIGURE 6: Rate of Ca^{2+} dissociation at an ATP concentration of 0.05 mM (circles) vs. 5 mM (squares), under two different conditions: In panel A, the experiment was performed at 5 °C in our standard potassium-free medium containing 150 mM Mes–Tris. In panel B, it was performed at 20 °C, and the medium contained 100 mM KCl, 50 mM Mes–Tris, and 20% v/v Me_2SO. In both cases, the medium also contained 20 mM Mg^{2+}, 0.1 mM $^{45}Ca^{2+}$, and 1 mM [^{3}H]sucrose, and the pH was 6. Experimental procedure was as in Figure 4.

from being responsible for slow Ca^{2+} release.

At 20 °C in the absence of potassium and Me_2SO, i.e. under our standard conditions, we repeated the experiment with ATP concentrations ranging from 0.02 to 10 mM (Figure 7A); the results suggest a rather low apparent affinity for ATP, around 0.5 or 1 mM. We also monitored ATP-induced Ca^{2+} dissociation with Antipyrylazo III. Figure 7B shows that optical detection and radioactivity measurements gave consistent data for different ATP concentrations. Apparent rate constants, however, were more easily deduced from the accumulated optical traces than from the ^{45}Ca measurements. A poor affinity was again found for the ATP-induced acceleration (see inset to panel B), confirming the rapid filtration data. Note that the k_{obsd} plotted in the inset slightly overestimates the true rate of the calcium-releasing transition, which is probably close to 3–5 s^{-1} at 0.05 mM ATP (see Appendix).

Steady-State [γ-^{32}P]ATP Binding to ^{32}P-Labeled Phosphoenzyme. The stimulation by ATP of the rate of the transition between the two phosphoenzyme forms prompted us to see whether there was any ATP binding to phosphorylated ATPase. This is shown in Figure 8A. After addition of various concentrations of [γ-^{32}P]ATP to the ATPase, the mixture was manually quenched with acid, and the covalently bound ^{32}P was determined by filtration on a glass fiber filter followed by thorough rinsing (closed symbols in Figure 8A). In a second set of experiments, the ^{32}P bound to the ATPase, either covalently or noncovalently, was determined by perfusing a Millipore filter and its adsorbed ATPase with various concentrations of ATP in the same medium as before, and subtracting the amount of [^{32}P]ATP trapped with water on the filter from the total amount of ^{32}P found on the filter (see Experimental Procedures). This subtraction was completely

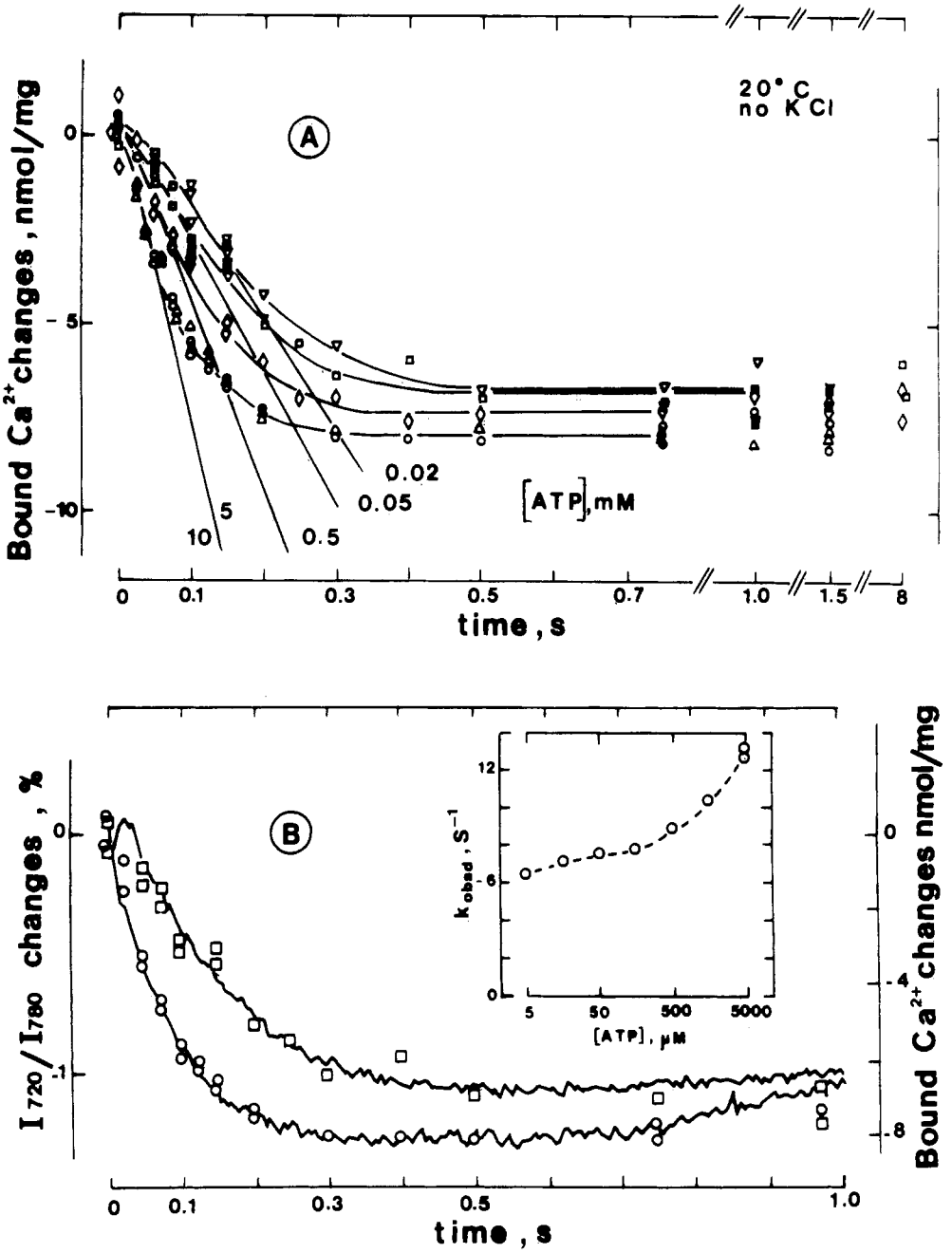

FIGURE 7: ATP dependence of the rate of Ca^{2+} dissociation. (Panel A) The medium contained 150 mM Mes–Tris (pH 6, 20 °C), 20 mM Mg^{2+}, 0.1 mM $^{45}Ca^{2+}$, 1 mM [^{3}H]sucrose, and an ATP concentration of 10 (triangles), 5 (circles), 0.5 (diamonds), 0.05 (squares), or 0.02 mM (upside-down triangles). Experimental procedure was as in Figure 4. (Panel B) ATP-induced absorbance changes in the presence of Antipyrylazo III. The medium contained 150 mM Mes–Tris, 20 mM Mg^{2+}, and 0.1 mM Antipyrylazo III (pH 6, 20 °C). The enzyme syringe of the Dionex stopped-flow spectrophotometer contained 0.6 mg/mL ATPase plus 4% w/w A_{23187}. The substrate syringe contained ATP. The dual-wavelength D-137 attachment was used. The Ca^{2+} concentration in the medium was 0.1 mM, and the ATP concentration after mixing was varied. Two examples are shown, respectively obtained at 0.05 (upper curve) and 5 mM (lower curves). The corresponding radioactive determinations taken from panel A are superimposed. Inset shows the ATP dependence of the rate constant of the observed signal drop (see, however, the Appendix).

reliable up to 0.5 mM ATP (where the "signal over noise" ratio was about 7/50) due to our using [^{3}H]sucrose as a marker of trapped volume; it became less reliable at 1 mM ATP. Nevertheless, ^{32}P binding clearly revealed a biphasic shape. The first phase, parallel to the curve of phosphoenzyme formation, depicted an affinity for ATP of a few micromoles per liter due to the particular experimental conditions used here (pH 6, 20 mM Mg^{2+}, no K^+). A secondary rise in ^{32}P binding took place with a much lower (millimolar?) affinity.

It might be argued that at the high ATP concentrations used this secondary rise reveals some kind of nonspecific binding. To rule out this possibility and simultaneously evaluate active site stoichiometry in our purified ATPase preparation, we repeated [^{32}P]ATP filtration experiments in the presence of the Ca^{2+} chelator EGTA (Figure 8B). Under these conditions, only binding of ATP took place without phosphorylation. At 0.5 mM ATP, bound ATP amounted to about 7 nmol/mg (panel B), i.e., significantly less than in the presence of calcium (panel A). At pH 6 and 20 mM Mg^{2+} (triangles in panel B), the affinity for ATP of the ATPase was poor (0.02 mM, a value consistent with unpublished fluorescence titrations by J.-J. Lacapère), so that the plateau level was not well-defined. In our experiment, we therefore included measurements of ATP binding in a more alkaline Ca^{2+}-deprived medium with

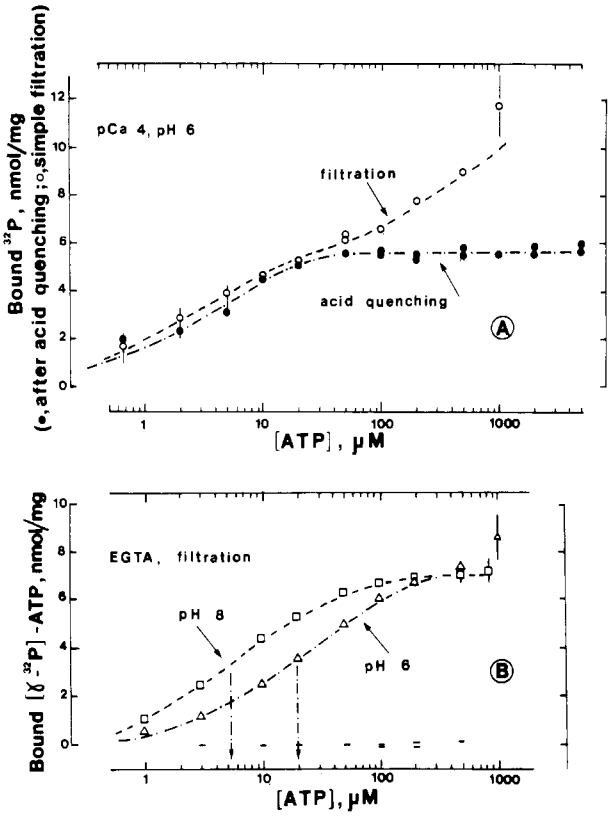

FIGURE 8: (Panel A) ^{32}P filtration experiments (EP + bound ATP) vs. acid-quenching experiments (EP) at steady state. The medium contained 150 mM Mes–Tris (pH 6, 20 °C), 20 mM Mg^{2+}, 0.1 mM Ca^{2+}, and various concentrations of [γ-^{32}P]ATP, added from a stock solution containing [^{3}H]sucrose. (Open symbols) Filtration experiments: a filter with adsorbed ATPase + 4% w/w A_{23187} was perfused with 0.5–5 mL of the solution containing ATP; 0.3 mg of ATPase was adsorbed on the filter, except for the lower ATP concentration for which this amount was reduced to 0.03 mg to prevent ATP depletion during the experiment. These experiments were conducted with two Millipore filters on top of each other. ATPase was only adsorbed on the upper one, in accordance with the method of Hasselbach and Koenig (1980), so that the lower one could be used to check the absence of nonspecific adsorption (not shown). (Closed symbols) Acid-quenching experiments: 0.1–33 mL of the solution containing ATPase, ionophore, and ATP was quenched after a few seconds with an equal volume of acid; 0.3 mg of ATPase was generally present, but this amount was reduced to 0.03 mg for the lowest ATP concentration, again in order to prevent ATP depletion during the experiment. (Panel B) Simple filtration experiments in the absence of calcium, designed to determine the amount of ATP bound by ATPase. The medium contained either 150 mM Mes–Tris, 20 mM Mg^{2+}, and 2 mM EGTA (pH 6, 20 °C, triangles) or 150 mM Tes–Tris, 2 mM Mg^{2+}, and 2 mM EGTA (pH 8, 20 °C, squares). A total of 0.2–10 mL of a solution containing various concentrations of [^{32}P]ATP + [^{3}H]sucrose was perfused through a double filter: the upper one contained 0.3 mg of ATPase and 4% w/w A_{23187}. In this same experiment, the amount of calcium passively bound under our standard conditions (pH 6, no K^+, 20 mM Mg^{2+}, 0.1 mM Ca^{2+}) was 13.5–14 nmol/mg (not shown).

a lower Mg^{2+} concentration (squares in panel B): under these conditions, the plateau was nicely defined and showed that the active site stoichiometry of our ATPase was about 7 nmol/mg. This value is consistent with the 11–15 nmol of calcium bound at the high-affinity transport sites (see above) and suggests that the secondary rise in ^{32}P binding in excess of 7 nmol/mg observed in the presence of calcium (Figure 8A) was due to low-affinity binding of [γ-^{32}P]ATP to the ^{32}P-labeled phosphoenzyme, rather than to some kind of nonspecific binding.

Dephosphorylation Rate Dependence on ATP and Mg^{2+}. The modulation by ATP of the rate of calcium dissociation from phosphorylated ATPase (Figures 6 and 7) implies ATP binding to the calcium-containing phosphoenzyme. On the other hand, it was previously suggested that ATP exerted its low-affinity modulatory role on overall ATP hydrolysis by stimulating deposphorylation, i.e., by interacting with the Ca^{2+}-free phosphoenzyme, E_2P in our scheme (Figure 1). Thus, in a Ca^{2+}-free medium, ATP perturbed the ATPase-mediated oxygen exchange between water and phosphate (McIntosh & Boyer, 1983). We therefore also tested under our experimental conditions the possible interaction between E_2P and high ATP concentrations by measuring the rate of E_2P dephosphorylation. Although a multimixer could have been used for this purpose, we again used the rapid filtration machine, and determined the amount of ^{32}P bound to the ATPase on the assumption that virtually all the ^{32}P bound to the ATPase under the conditions described below would be covalently bound, because the OFF rate for phosphate is very fast—faster than 100 s^{-1} at pH 6 in the absence of potassium (Guillain et al., 1984).

To facilitate phosphorylation, purified ATPase was first phosphorylated with [^{32}P]P_i in a Ca^{2+}-deprived medium containing Me_2SO, deposited on the filter, and perfused with different tracer-free mediums to initiate dephosphorylation. Panel C in Figure 9 shows that at pH 6 in the absence of potassium and in the presence of 20 mM Mg^{2+} (i.e., under conditions similar to those in Figure 7) the dephosphorylation rate was not stimulated by including 5 mM ATP in the dephosphorylation medium. In previous experiments with a multimixer and a different medium (pH 7 and no potassium), we had also found that the dephosphorylation rate was not affected by ATP addition in the presence of Mg^{2+} (Champeil et al., 1985).

However, when dephosphorylation was performed in the absence of magnesium in the present experiments at pH 6, ATP did accelerate dephosphorylation (see panel D in Figure 9, squares vs. circles), suggesting that metal-free ATP did interact with the magnesium-containing phosphoenzyme, more efficiently than the Mg–ATP complex; this is consistent with similar evidence for ATP interaction with the vanadate–ATPase complex (Andersen & Møller, 1985).

Note that in the absence of ATP magnesium per se had no effect on the ATPase dephosphorylation rate at pH 6 (panel A in Figure 9), in agreement with the assumed mechanism of phosphoenzyme formation [see similar data obtained at pH 7 in Champeil et al. (1985)]. This contrasts with the results observed at alkaline pH, where magnesium strongly inhibited this dephosphorylation rate (panel B in Figure 9), as previously reported by de Meis et al. (1980) and discussed below.

Maximal Phosphoenzyme Level vs. Active Site Concentration: ATP Modulation of Calcium-Induced Transition from E_2 to Ca_2E_1. Besides the demonstration of [^{32}P]ATP binding to ^{32}P-labeled phosphoenzyme, a puzzling feature emerged from the experiment depicted in Figure 8A,B, namely, the maximal amount of covalent phosphoenzyme was significantly lower than the titrated amount of ATP binding sites (slightly less than 6 nmol/mg, vs. about 7 nmol/mg). We do not think this is within the limits of experimental error. Possible explanations for this slight discrepancy include (i) the existence of a small proportion of ATPase that whould be partly denatured, with intact Ca^{2+} or ATP binding sites but reduced ability to be phosphorylated, (ii) the existence of a significant proportion of Ca_2E_1ATP complex, a precursor not explicitly included in our scheme (Shigekawa & Kanazawa, 1982; Pickart & Jencks, 1982), and (iii), in terms of our simple scheme, that this slight difference might mean that under these conditions a small amount of a nonphosphorylated form of

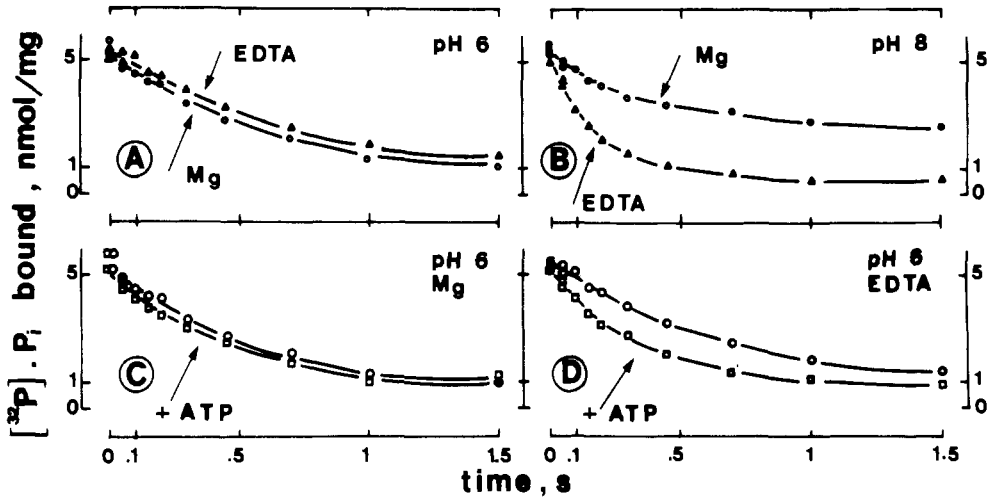

FIGURE 9: E_2P to E_2 dephosphorylation in various mediums. Phosphoenzyme was formed by incubating 0.3 mg/mL purified ATPase in a solution containing 115 mM Mes–Tris (pH 6, 20 °C), 15% v/v Me_2SO, 20 mM Mg^{2+}, 2 mM EGTA, 1 mM [^{3}H]sucrose, and 0.2 mM [^{32}P]P_i; 1 mL of this suspension was layered on a filter, which was then perfused for predetermined periods with various dephosphorylation mediums. (Panels A and B) Effect of Mg^{2+} on the dephosphorylation rate. In panel A, the dephosphorylation medium contained 150 mM Mes–Tris (pH 6, 20 °C) and either 20 mM Mg^{2+} (circles) or 5 mM EDTA (triangles). In panel B, the dephosphorylation medium contained 150 mM Tricine–Tris (pH 8, 20 °C) and either 10 mM Mg^{2+} (circles) or 10 mM EDTA (triangles). (Panels C and D) Effect of ATP on the dephosphorylation rate. The dephosphorylation medium contained 150 mM Mes–Tris (pH 6, 20 °C). In addition, in panel C, it contained 20 mM Mg^{2+}, 2 mM EGTA, and either 0 (circles) or 5 mM ATP (squares), and in panel D, it contained 5 mM EDTA and either 0 (circles) or 5 mM ATP (squares). Here, the purified ATPase was not preincubated with ionophore. When the experiments were repeated in the presence of ionophore (data not shown), some ionophore-induced slowing down of the basal dephosphorylation rate was evidenced (see Experimental Procedures). In addition, as previously reported, the initial level of phosphoenzyme was higher (7 nmol/mg) when the ATPase had been preincubated with ionophore [see, for instance, Pick and Racker (1980)]. This is probably connected with our finding that the orientationally randomized ATPase preparation was not completely leaky, implying that some bound calcium ions were left in an EGTA-inaccessible compartment and precluding maximal phosphorylation in the absence of ionophore.

ATPase piled up at steady state. The Ca_2E_1 form was not likely to pile up to any degree since the phosphorylation reaction was fast (about 30 s^{-1} at 0.005 mM ATP, not shown). We therefore suspected that the E_2 form piled up, although the rate of the transition from E_2 to Ca_2E_1 had been shown to be accelerated by ATP (Scofano et al., 1979).

To check this possibility, we first performed a reference standard Ca^{2+} release experiment in the presence of a high ATP concentration, starting from a Ca^{2+}-saturated ATPase (open squares in Figure 10). In a second experiment, we started by perfusing the ATPase with an EGTA-containing solution in order to deplete the Ca^{2+} binding sites and then perfused this "E_2" ATPase with a solution containing ATP and the adequate final concentration of calcium (0.1 mM) for various periods. If the E_2 to Ca_2E_1 transition had been very fast, we should have observed an overshoot in the amount of bound ^{45}Ca, i.e., very fast binding of two calcium ions followed by the slower Ca^{2+}-releasing transition. The expected overshoot was definitely not observed (closed squares in Figure 10), implying that the transition from E_2 to Ca_2E_1 was only accelerated to a moderate extent (about 6 s^{-1}) by the high ATP concentration used and was therefore partially rate limiting for the complete cycle, thus resulting in the accumulation of a small but significant amount of the E_2 form under these experimental conditions (pH 6, no potassium, 20 °C). Similar results (not shown) were also obtained at pH 6 in the presence of potassium.

Discussion

Phosphorylation-Dependent Calcium Dissociation: General Features. The initial purpose of this investigation was to document the kinetic features of the Ca^{2+} dissociation which normally takes place on the luminal side of the sarcoplasmic reticulum calcium pump. Technical prerequisites for this study included (i) availability of completely leaky ATPase-containing membranes (in our hands this required the addition of ionophore, see Experimental Procedures) and (ii) availability of adequate methods to permit time-resolved measurements of the Ca^{2+} dissociation: in this respect, direct ^{45}Ca measurements with the Biologic rapid filtration system and dual-wavelength optical measurements with Antipyrylazo III and the Dionex D137 attachment gave consistent results (Figure 7A,B).

At pH 6 and 20 °C, the rate of the Ca^{2+}-releasing transition was moderately fast in the absence of potassium (between 3 and 5 s^{-1} at 0.05 mM ATP, see Figure 7 and Appendix); at pH 7 and 8 it was slightly stimulated, and at pH 6 in the presence of potassium it was slower by half (Figure 4); this K^+-induced slowing down of the transition from Ca_2E_1P to E_2P is in agreement with previous determinations at 0 °C (Yamaguchi & Kanazawa, 1985); when combined with the known K^+-induced acceleration of the dephosphorylation transition from E_2P to E_2, it accounts for the higher proportion of ADP-sensitive phosphoenzyme generally found at steady state in the presence of potassium [e.g., Shigekawa and Akowitz (1979)]. The slower transition to an ADP-insensitive form of a phosphoenzyme with three bound calcium ions (Shigekawa et al., 1983) was also confirmed (Figure 5).

pH Dependence of Steady-State Ca^{2+} Dissociation and Rate Limitation of the Cycle. The amount of calcium released at steady state under given experimental conditions reflects the proportion of ATPase molecules found under these conditions in one of the Ca^{2+}-deprived states (E_2 or E_2P) rather than in one of the Ca^{2+}-rich states (Ca_2E_1 or Ca_2E_1P). The extent of this release, i.e., the drop in the amount of Ca^{2+} bound to the ATPase after addition of ATP, is considerable if the late steps in the cycle (from E_2P to E_2 or from E_2 to Ca_2E_1) are rate-limiting, and therefore, its measurement provides some information about the relative rates of the various steps in the cycle.

The pH dependence of steady-state Ca^{2+} dissociation we observed (Figure 3) may be considered from this point of view.

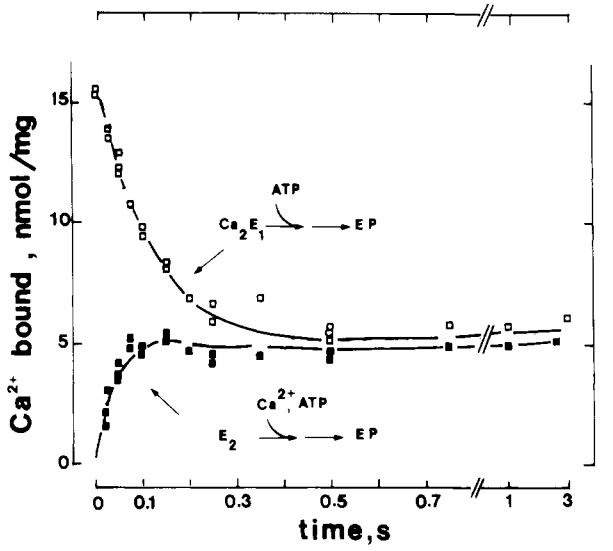

FIGURE 10: Calcium movements to and from the ATPase transport sites, in two different situations. In both cases, the perfusion medium contained 150 mM Mes–Tris (pH 6, 20 °C), 20 mM Mg^{2+}, 1 mM [^{3}H]sucrose, 0.1 mM $^{45}Ca^{2+}$, and 5 mM ATP; 1 mL of a suspension containing 0.3 mg/mL purified ATPase and A_{23187} (4% w/w ionophore/protein) in a similar ATP-free medium had been previously layered onto the Millipore filter. (Open squares) This initial ATPase suspension contained 1 mM [^{3}H]sucrose and 0.1 mM $^{45}Ca^{2+}$, as in most Ca^{2+} dissociation experiments in this work. (Closed squares) The purified ATPase, preincubated with 4% w/w A_{23187}, was first layered onto the filter and then deprived of calcium by preliminary washing with EGTA-containing solutions (0.05 mM EGTA for the last wash). Three control experiments for the Ca^{2+} dissociation curve (open squares) were also performed (data not shown): When a Ca^{2+} dissociation experiment was performed with native SR vesicles rendered leaky by inclusion of 4% w/w A_{23187}, the time course and amplitude of the observed release correlated adequately with those observed using purified ATPase. When a similar experiment was repeated with SR vesicles that had not been preincubated with ionophore, Ca^{2+} uptake was of course observed. When a similar experiment was performed with purified ATPase in the absence of ionophore, a certain proportion of the ATPase molecules did release their bound Ca^{2+}, but this release was soon obscured by residual uptake (see Experimental Procedures).

In the presence of Me_2SO (panel B), dephosphorylation was the slowest step in the cycle, and the E_2P phosphoenzyme piled up (Watanabe et al., 1981). In the absence of Me_2SO and potassium, at pH 6 and 20 °C (panel A), the dephosphorylation rate was still slow enough to be the main rate-limiting step [1.5–2.0 s^{-1} in the absence of ionophore and 1.0 s^{-1} in its presence; see Figure 9 and Guillain et al. (1984)], although the E_2 to Ca_2E_1 transition also contributed to rate limitation, even at high ATP concentrations (see Figure 10, squares). Note that under these conditions the maximal steady-state rate of P_i liberation was about 6 nmol/mg·s, consistent with the idea that most of the phosphoenzyme was present in the E_2P form.

When pH is shifted toward neutrality, the dephosphorylation rate rises from 1.5–2 s^{-1} to about 10 s^{-1} at pH 7 [see Champeil et al. (1985)], and the basal E_2 to Ca_2E_1 transition rate in the absence of ATP is also enhanced from 1.1–1.7 s^{-1} to 4–6 s^{-1} [see Guillain et al. (1981) and Champeil et al. (1983)]. Since these relatively large changes more than compensate the slight acceleration at pH 7 of the Ca^{2+}-releasing isomerization (from Ca_2E_1P to E_2P, Figure 4B), it is concluded that less Ca^{2+} must be released at pH 7 than at pH 6. We indeed found a smaller Ca^{2+} release at pH 7 than at pH 6, both in the absence (Figure 3A) and in the presence (Figure 3C) of potassium, in contrast with a previous report [Figure 3 in Andersen et al. (1985b)]. In our case, the addition of ionophore probably made the difference, since (i) it slightly slowed down the dephosphorylation rate, thereby helping E_2P to accumulate, and (ii) it prevented any possible residual calcium uptake at acidic pH from obscuring Ca^{2+} release.

In the presence of 100 mM potassium and 10 mM Mg^{2+} at pH 7, i.e., under the conditions most widely used, calcium release was hardly measurable (Figure 3C), suggesting that Ca_2E_1P piled up and that the transition from Ca_2E_1P to E_2P was rate-limiting. Under similar conditions, isomerization of the phosphorylated enzyme has been recognized to be the rate-limiting step in the cycle (Inesi et al., 1982). We recently also reached an identical conclusion by studying how low concentrations of a nonionic detergent perturbed the individual steps in the catalytic cycle as well as the overall hydrolysis rate (Champeil et al., 1986).

At alkaline pH, the rate of Ca^{2+} dissociation was not much changed (Figure 4B), but magnesium strongly inhibited the dephosphorylation rate [Figure 9B and de Meis et al. (1980)]. Therefore, E_2P again piled up, due to the now efficient stabilization of phosphoenzyme by magnesium, and a large extent of Ca^{2+} dissociation was observed at alkaline pH [Figure 3 and Andersen et al. (1985b)]. The Mg^{2+}-induced inhibition of ATPase dephosphorylation might be due to Mg^{2+} binding at alkaline pH to one or several "internal" calcium sites, thus depleting E_2P conformation (L. de Meis, personal suggestion).

ATP Modulation of the Rate of Ca^{2+} Dissociation. Figures 6 and 7 document the ATP-induced acceleration of the Ca^{2+} dissociation that we demonstrated here, at pH 6. This moderate but clear acceleration had not been directly evidenced before. In our view, it is consistent with the previous observation by Watanabe et al. (1981) that more Ca^{2+} was released at steady state in the presence of 1 mM ATP than at 0.2 mM (their Figure 7A), since the effects of high ATP concentrations documented elsewhere, i.e., acceleration of dephosphorylation from E_2P to E_2 and of transition from E_2 to Ca_2E_1, imply a trend toward a reduction in the proportion of Ca^{2+}-poor states rather than toward increased Ca^{2+} release.

In addition, if the Ca^{2+}-releasing phosphoenzyme isomerization from Ca_2E_1P is indeed the rate-limiting step under selected conditions, as discussed in the above section, this same step must be the target of any modulatory effect of ATP on overall ATPase activity. There is a paradox here: under one of the present conditions, i.e., in the absence of potassium at pH 6, we did experimentally demonstrate that ATP accelerated the rate of Ca^{2+} dissociation (Figures 6 and 7). However, Ca^{2+} dissociation was easily observed under these conditions because the rate-limiting step was the dephosphorylation step, and ATP acceleration of the nonlimiting Ca^{2+}-releasing isomerization did not affect the overall ATP hydrolysis rate. Since Mg·ATP failed to stimulate the dephosphorylation rate at pH 6 in the absence of potassium (Figure 9C), low-affinity acceleration of overall ATP hydrolysis was therefore not observed under these conditions [data in Champeil et al. (1986)]. Conversely, in the presence of potassium at neutral pH, the well-known low-affinity stimulation of ATP hydrolysis must reflect acceleration by ATP of the rate-limiting Ca^{2+}-releasing isomerization, but under these conditions, experimental demonstration of the crucial ATP-induced stimulation of the rate of Ca^{2+} dissociation would be hampered by vanishing amplitude since the Ca^{2+}-free E_2P species does not pile up.

ATP Stimulation of Various Steps in the Cycle, with Special Reference to Magnesium. A general conclusion that emerges from the present investigation is that ATP not only affects phosphorylation but also all the intermediate steps in the catalytic cycle (Figure 1), including isomerization of phosphorylated ATPase, dephosphorylation, and isomerization

of nonphosphorylated ATPase. From a mechanistic point of view, this implies that after ADP departure ATP reenters the catalytic cycle long before rebinding of cytoplasmic calcium. The degree to which the regulation of one particular step is reflected in the overall ATP hydrolysis rate depends on the precise experimental conditions, which determine which step contributes most to rate limitation. In fact, an outcome of the present determination of the rates of the different steps is that under many steady-state conditions none of them is really very much slower than the others, so that the ATPase is likely to be found in various coexisting forms rather than in one overwhelmingly dominant form.

The regulatory effect of ATP on the dephosphorylation step was highly dependent on magnesium under our experimental conditions. Thus, we found here that, at pH 6 in the absence of potassium, 5 mM ATP did not stimulate the dephosphorylation rate in the presence of 20 mM Mg^{2+}, whereas it did in the presence of EDTA (Figure 9C,D). This contrasts with other reports (McIntosh & Boyer, 1983). We suggest that free ATP and Mg·ATP do not accelerate the deposphorylation step to the same degree. This might also apply to the other steps and might partly account for the fact that ATP accelerates ATPase activity to a lesser degree in a medium containing a high Mg^{2+} concentration than in a medium containing a lower concentration [e.g., in Champeil et al. (1986)]. This is also reminiscent of a previous report showing preferential binding of ATP rather than of Mg·ATP to the vanadate–ATPase complex, also believed to contain magnesium at the active site (Andersen & Møller, 1985).

On the other hand, in the presence of 20 mM magnesium, high concentrations of ATP did accelerate processing of the calcium-containing phosphoenzyme (Figures 6 and 7), which therefore efficiently interacts with Mg·ATP. In the calcium-containing phosphoenzyme (as opposed to the Ca^{2+}-deprived phosphoenzyme), an apparent diminution in the repulsive interaction between the nucleotide-complexed magnesium and the magnesium in the catalytic cycle would be consistent with a previous suggestion by Wakabayashi and Shigekawa (1984): according to these authors, the metal ion in the catalytic cycle is exchangeable in the Ca_2E_1P phosphoenzyme, whereas it cannot be extracted from the Ca^{2+}-deprived E_2P phosphoenzyme [as also evidenced by the fact that hydrolysis of E_2P at pH 6 (Figure 9A) was insensitive to the presence of EDTA in the dephosphorylating medium].

Our data about ATP acceleration of the various transition rates do not at present enable us to decide whether ATP binding to phosphoenzyme takes place at a regulatory site or at the catalytic site after ADP elimination [a widely discussed issue: see Bishop et al. (1984), Nakamoto and Inesi (1984), Dupont et al. (1985), Cable et al. (1985), Coll and Murphy (1985), and Taylor and Hattan (1979)]. We, however, favor the second possibility because of the Mg^{2+} sensitivity just mentioned (panels C and D in Figure 9), because of the stoichiometry revealed by ATP binding in the absence of calcium (Figure 8B), and because of the results of recent studies with labeled TNP nucleotides (Davidson and Guillain, unpublished results) and with FITC-modified ATPase (Riollet, Champeil, and Guillain, unpublished results).

It should also be noted that we did not attempt to resolve the "calcium releasing isomerization" from Ca_2E_1P to E_2P into further substeps, as recently attempted elsewhere (Froehlich & Heller, 1985; Andersen et al., 1985a). ATP might either accelerate the rate of phosphoenzyme isomerization (from Ca_2E_1P to Ca_2E_2P) or accelerate calcium dissociation from the calcium-containing phosphoenzyme (Ca_2E_2P).

ACKNOWLEDGMENTS

We are heavily indebted to Jesper V. Møller and Jens P. Andersen for initial impetus to investigate calcium release and subsequent long-lasting discussions. We thank J. J. Lacapère for cooperation and Mathilde Dreyfus and Patricia Belle for their help in editing and typing the manuscript.

APPENDIX

Note that the observed rate constant plotted in the inset to Figure 7B is the rate constant of the exponential that adequately describes the absorbance drop, i.e., it is related to the half-time ($t_{1/2}$) of this drop by the relation k_{obsd} (s^{-1}) = $0.69/t_{1/2}$ (s). This observed rate constant is *not* the true rate constant of the transition from Ca_2E_1P to E_2P but is *higher* than the latter, because at steady state all the enzyme is not found in the E_2P state but part of it is recycled toward Ca_2E_1P through the late steps in the cycle (Figure 1). This is analogous to what is found in a reversible transition from A to B ($A \underset{k_-}{\overset{k_+}{\rightleftharpoons}} B$), where the observed rate at which the equilibrium is reached not only depend on k_+ but also includes a contribution from the reverse rate k_-: $1/t_{1/2} = k_{obsd} = k_+ + k_-$. In principle, the true Ca_2E_1P to E_2P rate can be deduced by dividing the *initial* rate of Ca^{2+} release by the concentration of the Ca_2E_1P species. This is why the value we give for the Ca_2E_1P to E_2P rate constant (3–5 s^{-1} at 0.05 mM ATP) is smaller than the observed rate constant plotted in the inset to Figure 7B.

Registry No. ATP, 56-65-5; ATPase, 9000-83-3; Ca, 7440-70-2; K, 7440-09-7.

REFERENCES

Andersen, J. P., & Møller, J. V. (1985) *Biochim. Biophys. Acta 815*, 9–15.

Andersen, J. P., Jørgensen, P. L., & Møller, J. V. (1985a) *Proc. Natl. Acad. Sci. U.S.A. 82*, 4573–4577.

Andersen, J. P., Lassen, K., & Møller, J. V. (1985b) *J. Biol. Chem. 260*, 371–380.

Bishop, J. E., Johnson, J. D., & Berman, M. C. (1984) *J. Biol. Chem. 259*, 15163–15171.

Cable, M. B., Feher, J. J., & Briggs, F. N. (1985) *Biochemistry 24*, 5612–5619.

Champeil, P., & Guillain, F. (1986) *Biophys. J. 49*, 568a.

Champeil, P., Gingold, M. P., Guillain, F., & Inesi, G. (1983) *J. Biol. Chem. 258*, 4453–4458.

Champeil, P., Guillain, F., Venien, F., & Gingold, M. (1985) *Biochemistry 24*, 69–81.

Champeil, P., le Maire, M., Andersen, J. P., Guillain, F., Gingold, M., Lund, S., & Møller, J. V. (1986) *J. Biol. Chem.* (in press).

Coll, R. J., & Murphy, A. J. (1985) *FEBS. Lett. 187*, 131–134.

Dean, W. L., & Gray, R. D. (1983) *Biochemistry 22*, 515–519.

De Meis, L., & Vianna, A. L. (1979) *Annu. Rev. Biochem. 48*, 275–292.

De Meis, L., Martins, O. B., & Alves, E. W. (1980) *Biochemistry 19*, 4252–4261.

De Souza, D. G., & de Meis, L. (1976) *J. Biol. Chem. 251*, 6355–6359.

Dupont, Y. (1980) *Eur. J. Biochem. 109*, 231–238.

Dupont, Y. (1984) *Anal. Biochem. 142*, 504–510.

Dupont, Y., Bennett, N., Pougeois, R., & Lacapere, J.-J. (1985a) in *Structure and Function of Sarcoplasmic Reticulum* (Tonomura, Y., & Fleischer, S., Eds.) pp 225–248, Academic, New York.

Dupont, Y., Pougeois, R., Ronjat, M., & Verjovski-Almeida, S. (1985b) *J. Biol. Chem. 260*, 7241–7249.

Fernandez-Belda, F., Kurzmack, M., & Inesi, G. (1984) *J. Biol. Chem. 259*, 9687–9698.
Froehlich, J. P., & Eller, P. F. (1985) *Biochemistry 24*, 126–136.
Guillain, F., Champeil, P., Lacapere, J.-J., & Gingold, M. P. (1981) *J. Biol. Chem. 256*, 6140–6147.
Guillain, F., Gingold, M. P., & Champeil, P. (1982) *J. Biol. Chem. 257*, 7366–7371.
Guillain, F., Champeil, P., & Boyer, P. D. (1984) *Biochemistry 23*, 4754–4761.
Hasselbach, N., & Koenig, V. (1980) *Z. Naturforsch. C: Biosci. 35C*, 1012–1018.
Ikemoto, N. (1975) *J. Biol. Chem. 250*, 7219–7224.
Inesi, G., Kurzmack, M., Kosk-Kosicka, D., Lewis, D., Scofano, H., & Guimaraes-Motta, H. (1982) *Z. Naturforsch. C: Biosci. 37C*, 685–691.
Makinose, M. (1973) *FEBS Lett. 37*, 140–143.
McIntosh, D. B., & Boyer, P. D. (1983) *Biochemistry 22*, 2867–2875.
McIntosh, D. B., & Davidson, G. A. (1984) *Biochemistry 23*, 1959–1965.
Meissner, G., Conner, G. E., & Fleischer, S. (1973) *Biochim. Biophys. Acta 298*, 246–269.
Nakamoto, R. K., & Inesi, G. (1984) *J. Biol. Chem. 259*, 2961–2970.
Nakamura, J. (1983) *Biochim. Biophys. Acta 723*, 182–190.
Nakamura, Y., & Tonomura, Y. (1982) *J. Biochem. (Tokyo) 91*, 449–461.
Pick, U., & Racker, E. (1979) *Biochemistry 18*, 108–113.
Pickart, C. M., & Jencks, W. P. (1982) *J. Biol. Chem. 257*, 5319–5322.
Scofano, H. M., Vieyra, A., & de Meis, L. (1979) *J. Biol. Chem. 254*, 10227–10231.
Shigekawa, M., & Dougherty, J. P. (1978) *J. Biol. Chem. 253*, 1458–1464.
Shigekawa, M., & Akowitz, A. A. (1979) *J. Biol. Chem. 254*, 4726–4730.
Shigewaka, M., & Kanazawa, T. (1982) *J. Biol. Chem. 257*, 7657–7665.
Shigewaka, M., Wakabayashi, S., & Nakamura, H. (1983) *J. Biol. Chem. 258*, 14157–14161.
Takisawa, H., & Tonomura, Y. (1979) *J. Biochem. (Tokyo) 86*, 425–441.
Takisawa, H., & Makinose, M. (1983) *J. Biol. Chem. 258*, 2986–2992.
Taylor, J. S., & Hattan, D. (1979) *J. Biol. Chem. 254*, 4402–4407.
Watanabe, T., Lewis, D., Nakamoto, R., Kurzmack, M., Fronticelli, C., & Inesi, G. (1981) *Biochemistry 20*, 6617–6625.
Yamada, S., & Ikemoto, N. (1980) *J. Biol. Chem 255*, 3108–3119.
Yamaguchi, M., & Kanazawa, T. (1984) *J. Biol. Chem. 259*, 9526–9531.
Yamaguchi, M., & Kanazawa, T. (1985) *J. Biol. Chem. 260*, 4896–4900.

Site-Specific Photo-Cross-Linking Studies on Interactions between Troponin and Tropomyosin and between Subunits of Troponin†

Terence Tao,* Cathy J. Scheiner, and Mark Lamkin
Department of Muscle Research, Boston Biomedical Research Institute, Boston, Massachusetts 02114, and Department of Neurology, Harvard Medical School, Boston, Massachusetts 02115

Received April 9, 1986; Revised Manuscript Received July 31, 1986

ABSTRACT: We have used the sulfhydryl-specific heterobifunctional photo-cross-linker 4-maleimidobenzophenone (BP-Mal) to study the interactions of rabbit skeletal tropomyosin with troponin and of the troponin subunits with each other. We found that α,α-tropomyosin specifically labeled at Cys-190 with BP-Mal photo-cross-links with all three subunits of troponin with decreasing cross-linking yields in the order of troponin T, troponin I, and troponin C. There was no apparent Ca^{2+} dependence in the cross-linking yields. In separate experiments, we found that troponin C labeled specifically at Cys-98 with BP-Mal photo-cross-links to both troponin I and troponin T in the two binary complexes, as well as in the ternary complex. Again, no Ca^{2+}-dependent changes in the cross-linking yields were detectable. These results are in general agreement with the picture that troponin I and troponin T are in close contact with troponin C near its Cys-98 and that all three troponin subunits are in the proximity of Cys-190 of tropomyosin.

Although it is well established that the contraction of mammalian skeletal muscle is regulated by calcium ions (Ebashi et al., 1969), the molecular mechanism of this process is still not completely understood. It is known that the regulatory proteins troponin (Tn)[1] and tropomyosin (Tm) in the thin filament are involved and that inhibition of actomyosin ATPase activity is reversed when Ca^{2+} is bound to the TnC component of Tn. One model proposes that the binding of

† Supported by a grant from the National Institutes of Health (AM21673). Presented in preliminary form at the 28th Meeting of the Biophysical Society (Tao et al., 1984) and at the Biophysical Discussions, Nov 1985 (Tao et al., 1986).

* Address correspondence to this author at the Department of Muscle Research, Boston Biomedical Research Institute, 20 Staniford St., Boston, MA 02114.

[1] Abbreviations: Tn and Tm, rabbit skeletal troponin and tropomyosin, respectively; TnC, TnI, and TnT, Ca^{2+} binding, inhibitory, and Tm binding subunits of Tn, respectively; S1, chymotryptic myosin subfragment 1; BP-Mal, 4-maleimidobenzophenone; AGTC, *N*-[(4-azidobenzoyl)glycyl]-*S*-(2-thiopyridyl)cysteine; BP-Tm, $\alpha\alpha$Tm labeled at Cys-190 with BP-Mal; BP-TnC, TnC labeled at Cys-98 with BP-Mal; Hepes, *N*-(2-hydroxyethyl)piperazine-*N*′-2-ethanesulfonic acid; DTT, dithiothreitol; SDS, sodium dodecyl sulfate; EDTA, ethylenediaminetetraacetic acid; GdmCl, guanidinium chloride; EGTA, ethylene glycol bis(β-aminoethyl ether)-*N*,*N*,*N*′,*N*′-tetraacetic acid.

0006-2960/86/0425-7633$01.50/0